

In operando observation system for electrochemical reaction by soft X-ray absorption spectroscopy with potential modulation method

Masanari Nagasaka, Hayato Yuzawa, Toshio Horigome, and Nobuhiro Kosugi

Citation: *Review of Scientific Instruments* **85**, 104105 (2014); doi: 10.1063/1.4898054

View online: <http://dx.doi.org/10.1063/1.4898054>

View Table of Contents: <http://scitation.aip.org/content/aip/journal/rsi/85/10?ver=pdfcov>

Published by the [AIP Publishing](#)

Articles you may be interested in

Novel spectro-electrochemical cell for in situ/operando observation of common composite electrode with liquid electrolyte by X-ray absorption spectroscopy in the tender X-ray region

Rev. Sci. Instrum. **85**, 084103 (2014); 10.1063/1.4891036

An ultra-high vacuum electrochemical flow cell for in situ/operando soft X-ray spectroscopy study

Rev. Sci. Instrum. **85**, 043106 (2014); 10.1063/1.4870795

Fe diffusion, oxidation, and reduction at the CoFeB/MgO interface studied by soft x-ray absorption spectroscopy and magnetic circular dichroism

Appl. Phys. Lett. **96**, 092501 (2010); 10.1063/1.3332576

Pt metal- CeO₂ interaction: Direct observation of redox coupling between Pt⁰ / Pt²⁺ / Pt⁴⁺ and Ce⁴⁺ / Ce³⁺ states in Ce_{0.98}Pt_{0.02}O_{2-δ} catalyst by a combined electrochemical and x-ray photoelectron spectroscopy study

J. Chem. Phys. **130**, 114706 (2009); 10.1063/1.3089666

Depth profile of alloying extent and composition in bimetallic nanoparticles investigated by in situ x-ray absorption spectroscopy

Appl. Phys. Lett. **91**, 023108 (2007); 10.1063/1.2755876



NEW
Model PS-100
Tabletop Cryogenic
Probe Station

Lake Shore
CRYOTRONICS

*An affordable solution for
a wide range of research*

In operando observation system for electrochemical reaction by soft X-ray absorption spectroscopy with potential modulation method

Masanari Nagasaka,^{1,2,a)} Hayato Yuzawa,¹ Toshio Horigome,¹ and Nobuhiro Kosugi^{1,2}

¹Institute for Molecular Science, Myodaiji, Okazaki 444-8585, Japan

²The Graduate University for Advanced Studies, Myodaiji, Okazaki 444-8585, Japan

(Received 22 August 2014; accepted 2 October 2014; published online 17 October 2014)

In order to investigate local structures of electrolytes in electrochemical reactions under the same scan rate as a typical value 100 mV/s in cyclic voltammetry (CV), we have developed an *in operando* observation system for electrochemical reactions by soft X-ray absorption spectroscopy (XAS) with a potential modulation method. XAS spectra of electrolytes are measured by using a transmission-type liquid flow cell with built-in electrodes. The electrode potential is swept with a scan rate of 100 mV/s at a fixed photon energy, and soft X-ray absorption coefficients at different potentials are measured at the same time. By repeating the potential modulation at each fixed photon energy, it is possible to measure XAS of electrochemical reaction at the same scan rate as in CV. We have demonstrated successful measurement of the Fe L-edge XAS spectra of aqueous iron sulfate solutions and of the change in valence of Fe ions at different potentials in the Fe redox reaction. The mechanism of these Fe redox processes is discussed by correlating the XAS results with those at different scan rates.

© 2014 AIP Publishing LLC. [<http://dx.doi.org/10.1063/1.4898054>]

I. INTRODUCTION

The electrochemical reaction occurs at the solid-liquid interface between the electrode surface and the liquid electrolyte. The mechanism of the electrochemical reaction has been mainly investigated by cyclic voltammetry (CV) measurements. In order to understand the electrochemical reaction more precisely, however, it is necessary to investigate local structural changes of electrolytes including electric double layers in the electrochemical reaction by using *in operando* spectroscopic techniques that can measure the reaction at the same condition as in CV. X-ray absorption spectroscopy (XAS) of core electron regions is an element specific method to study local electronic structures and is applicable to liquid samples as well as gas and solid samples. Especially, the soft X-ray region below 1 keV has many chemically important core levels such as C, N, and O K-edges. Recently, the structure of liquid water has been extensively studied by the O K-edge XAS.¹⁻³ The transmission mode is a quantitative method to measure the absolute photoabsorption cross section. XAS spectra of liquid samples can be measured by various methods, not only transmission mode^{4,5} but also fluorescence yield,² nonresonant Raman scattering process,³ total electron yield of liquid microjet,¹ and inverse partial fluorescence yield of liquid microjet.⁶⁻⁹ The latter methods are based on secondary processes, proportional to the probability of the core hole creation following the X-ray absorption. Their compatibility with the transmission measurement has been discussed as regards background subtraction, normalization, and saturation correction. Note that XAS in bulk liquid phase measured by the nonresonant Raman scattering and the inverse partial fluorescence yield is nearly the same as XAS in transmission mode. For the XAS measurement in trans-

mission mode, however, it is necessary to keep the thickness of the liquid layer below a few micrometers because soft X-rays are strongly absorbed by solvent molecules.^{5,10} Recently, we have successfully developed a liquid flow cell for XAS in transmission mode.⁴ The liquid layer is sandwiched between two Si₃N₄ membranes under atmospheric condition and the thickness of the liquid layer is controllable between 20 nm and 2000 nm. This liquid cell is also applicable to the XAS measurement of solid-liquid interface by depositing a solid substrate on the membrane and adjusting the thickness of the liquid layer as small as possible.

Furthermore, we have developed an *in situ* XAS measurement system to study local structures of electrolytes in electrochemical reaction by using a transmission-type liquid cell with built-in electrodes. Change in valence of Fe ions in an aqueous iron sulfate solution at different potentials is investigated by Fe L-edge XAS spectra.¹¹ Each Fe L-edge XAS spectrum is measured at a constant potential and the potential is changed to the next one after finishing each XAS measurement. As a result, the scan rate of the potential corresponds to 0.08 mV/s and is quite slower than a typical scan rate of 100 mV/s in CV. CV is not applicable in such slow scan rate, and the valence of Fe ions reaches the equilibrium at each potential. Therefore, this XAS measurement is not able to investigate kinetics of the electrochemical reaction. In order to investigate the kinetics of electrochemical reaction under realistic conditions, it is necessary to develop an *in operando* observation system that is able to measure XAS of electrolytes at the same scan rate as in CV.

The local structures of electrolytes in electrochemical reactions have been investigated by several spectroscopic techniques. Endo *et al.* studied adsorption structures of Br ions on Ag(100) surfaces at different potentials in aqueous NaBr solutions by measuring Br K-edge XAS in the hard X-ray region.¹² Bora *et al.* developed an *in situ* electrochemical

^{a)}Electronic mail: nagasaka@ims.ac.jp

reaction for XAS in fluorescence yield.¹³ Masuda *et al.* developed an hard X-ray photoelectron spectroscopy apparatus for *in situ* electrochemical reaction of solid-liquid interface and investigated potential-induced Si oxide growth in water at the Si membrane surface.¹⁴ The structures of solvent water molecules at different potentials were determined from the OH stretching mode in Fourier transform infrared spectroscopy.^{15,16} The adsorption structures of water molecules were studied by methods focusing on solid-liquid interfaces, such as sum frequency generation¹⁷ and surface-enhanced Raman spectroscopy.¹⁸ X-ray scattering study revealed that the orientation of water molecules at the first layer of Ag(111) electrodes is changed at different potentials in 0.1 M NaF.¹⁹ Wu *et al.* used Cu K-edge XAS to investigate the effect of different anions on the structure of underpotential deposition of Cu on Au.^{20,21} The *in situ* spatial measurements by scanning transmission X-ray microscope also applied to the electrochemical reaction.^{22,23} These spectroscopic methods revealed the local structures of electrolytes and solid-liquid interfaces at electrodes in electrochemical reactions. However, these measurements were performed at a constant potential and the potential is stepwise changed in electrochemical reactions. The scan rate of the potential is too slow to study the electrochemical reaction under the same scan rate as in CV.

In order to solve the above problem, it is necessary to develop the spectroscopic technique that is able to sweep the electrode potential at the same scan rate as in CV. Several groups tried to study the electrochemical reaction under the same scan rate as in CV. Ataka *et al.* studied the structures and orientations of water molecules adsorbed on Au(111) electrodes at different potentials in perchloric acid solutions by surface-enhanced infrared absorption spectroscopy at 5 mV/s.²⁴ Kunimatsu *et al.* studied the adsorption and oxidation of a methanol molecule on a platinum electrode in perchloric acid solutions containing methanol during electrochemical reaction by attenuated total reflectance Fourier transform infrared reflection absorption spectroscopy at 5 mV/s.²⁵ The structural changes of electrode surfaces in electrochemical reactions were studied by *in situ* surface X-ray diffraction at several mV/s.^{26,27} Braunschweig *et al.* studied the surface transformation of sulfate anions on Pt(111) surfaces during the electrochemical reaction of sulfuric acid solutions by sum-frequency generation at 5 mV/s.²⁸ As described above, there are several spectroscopic studies to measure electrochemical reactions at several mV/s, but it is still slower than a typical scan rate of 100 mV/s in CV. There are few studies to observe the electrochemical reaction at 100 mV/s and to study the local structures of electrolytes and solid-liquid interfaces at electrodes in electrochemical reaction by element-specific spectroscopy.

In the present study, we have developed an *in operando* observation system for electrochemical reactions under the same scan rate as in CV by XAS with a potential modulation method. This method is based on *in situ* XAS measurement system for electrochemical reaction recently developed by the present author group.¹¹ By using the present system, we have measured the potential-modulated Fe L-edge XAS spectra of aqueous iron sulfate solutions in electrochemical

reactions at 50 mV/s and 100 mV/s and discussed the change in valence of Fe ions in the Fe redox reaction at the different scan rates. The Fe L-edge (700 eV) is in the soft X-ray region below 1 keV and is more sensitive to the 3d valence and spin states of Fe ions than the Fe K-edge.^{11,29–31} Since XAS is an element-selective method to study local structures of liquid, *in operando* XAS with potential modulation has an advantage to investigate not only change in valence of ions but also the local structural changes of molecules, such as adsorption structures of water in electric double layers, in electrochemical reaction.

II. DESIGN OF INSTRUMENTATION

Figure 1 shows a schematic of the present *in operando* observation system for electrochemical reactions by potential-modulated XAS. The experiments were performed on the soft X-ray undulator beamline BL3U at the UVSOR-III facility.³² Section II A describes some details of the electrochemical cell for XAS in transmission mode. Section II B explains the *in operando* observation system for the electrochemical reaction by XAS with a potential modulation method.

A. Electrochemical cell

Figure 1(a) shows schematics of the liquid flow cell for XAS in transmission mode. As previously described,^{4,11,33} the liquid flow cell consists of four regions (I), (II), (III), and (IV), separated by 100 nm-thick Si₃N₄ membranes (NTT AT). SiC membranes (NTT AT) are used for the N K-edge measurement. Region (I) is connected to the beamline under vacuum. Regions (II) and (IV) are under atmospheric pressure of helium buffer gas. The size of the Si₃N₄ membrane window between regions (I) and (II) is 0.2 mm × 0.2 mm, which is small enough to endure a large difference in pressure, even larger than 1 atm. The size of the soft X-ray beam on the sample is determined by this orifice. The flow rate of the helium gas (and other gases) in the regions (II) and (IV) is changeable by a mass flow controller (Kofloc), and the pressure (if necessary larger than 1 atm) is adjusted by a needle valve at the gas outlet.

The thin liquid layer in the region (III) is sandwiched between two 100 nm-thick Si₃N₄ membranes with a window size of 2 mm × 2 mm. The liquid flow is under atmospheric condition. Two 100 μm-thick spacers are set between the window frames of the membranes and the membranes are compressed by sealing o-rings to keep the thin liquid layer below 2000 nm. Liquid samples can be exchanged *in situ* with a tubing pumping system (Cole-Parmer Masterflex L/S). The thickness of the liquid layer is controllable between 20 nm and 2000 nm by changing the He pressure in the regions (II) and (IV).^{4,11} Although the thickness of the liquid layer varies at different positions over the 2 mm × 2 mm membranes, it is possible to measure XAS of the liquid layer at a constant thickness because of the small beam size. In order to investigate electrochemical reactions, three electrodes are included in the liquid layer (III).¹¹ The working electrode (WE) is a gold deposited Si₃N₄ membranes, which consists of Au (20 nm), Cr (5 nm), and Si₃N₄ (100 nm) multilayer films. One

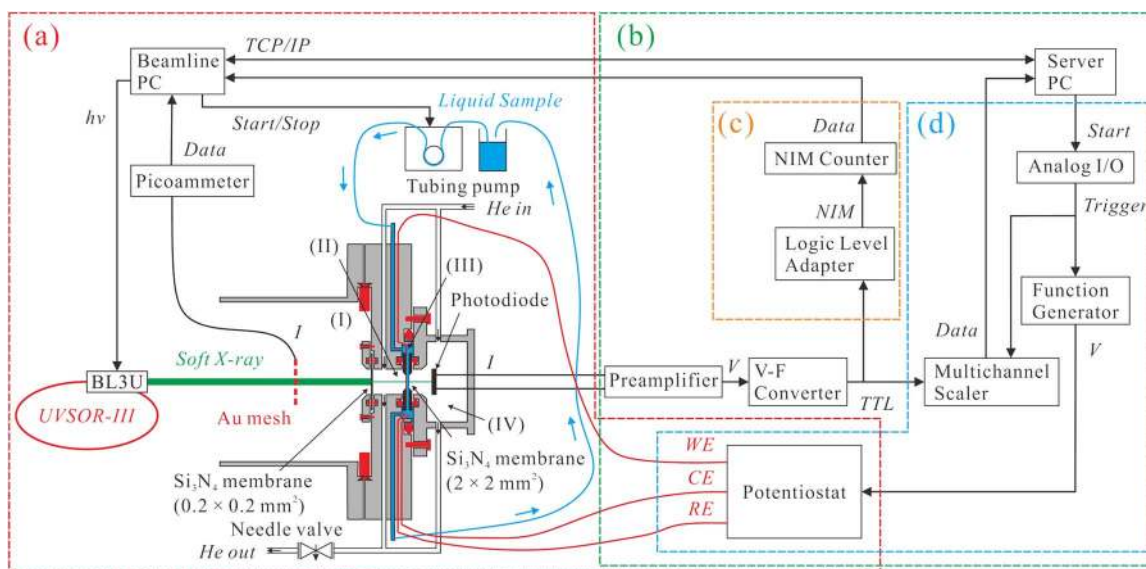


FIG. 1. Schematic of the *in operando* observation system for the electrochemical reaction by XAS with a potential modulation method. (a) The electrochemical cell for XAS in transmission mode. (b) The XAS measurement system with potential modulation method. (c) The data acquisition system for the reference XAS spectra. (d) The data acquisition system for the XAS spectra in electrochemical reaction at same scan rate as in CV.

side of this membrane faces the liquid layer (III) and is connected with the Au tab for electrical conduction. The Teflon spacer is placed on the Si frame, opposite the Au contact. The counter electrode (CE) is a Pt mesh, which is immersed in a sample electrolyte solution. The reference electrode (RE) is Ag/AgCl immersed in a saturated KCl solution and isolated from the liquid sample by a Teflon cover. The sample electrolyte solution is completely isolated from the ground. The potential is controlled by using a potentiostat (Solartron 1287).

Soft X-rays pass through the regions (I), (II), and (III) and are detected by a photodiode (IRD AXUV100) in the region (IV). The intensity of soft X-ray is normalized by an electric current of a gold mesh in the region (I), where the current is proportional to the photon flux and is measured by a picoammeter (Keithley 6514/J). The absorption of soft X-rays in regions (II) and (IV) is small due to the high transmittance of helium.¹⁰ The XAS spectra are obtained from the measured transmission signal at different photon energies, by using the Lambert-Beer formula $\ln(I_0/I)$, in which the current I_0 is measured for the blank and the current I is for the liquid sample.

B. System for potential modulation method

In the present potential-modulated XAS, the electrode potential is swept at a fixed photon energy and the soft X-ray absorption coefficients at different potentials are measured at the same time and is able to measure XAS of electrochemical reactions at the same scan rate as in CV. Figure 1(b) shows a schematic of this system. In order to perform time-resolved measurements of soft X-ray absorption coefficients, the electric currents obtained by the photodiode detector are amplified as voltages by a preamplifier (NF LI-76), and the voltages are converted to TTL signals by using a V-F converter (Tsuji-con SN2VF-01). Figure 1(c) shows the data acquisition system for the reference XAS spectrum that is not de-

pendent on the reaction time. When measuring the reference XAS spectrum, the TTL signals are converted to NIM signals by a logic level adapter (Kaizu Works KN200), and the NIM signals are counted by a NIM counter (Ortec 974). Figure 1(d) shows the data acquisition system for XAS in the electrochemical reaction. When measuring XAS spectra in the electrochemical reaction, the TTL signals at different elapsed times are accumulated in order with a constant dwell time by using a multichannel scaler (Ortec EASY-MCS). It is necessary to synchronize the start of the soft X-ray absorption measurement with that of the potential modulation. The measurement by the multichannel scaler is started by receiving a TTL trigger signal generated by an analog I/O (NI USB-6259). The trigger signal is received at the same time by a function generator (NF WF1974), which generates the potential curve of CV. By entering the generated potential curve to the external potential input in the potentiostat, the electrode potential is controlled in the electrochemical cell.

When the measurement of soft X-ray absorption coefficients during the potential modulation at a fixed photon energy is finished, the server PC controlling the potential-modulated measurements communicates with the beamline PC via a TCP/IP network. Then, the beamline PC changes the photon energy to the next one. The liquid sample is replaced by the fresh one at the same time by starting the tubing pump. The bottle of the liquid sample is bubbled by helium gas in order to remove dissolved oxygen. After setting the next photon energy, the measurement of soft X-ray absorption coefficients with the potential modulation is started by communicating with the server PC via a TCP/IP network.

III. RESULTS AND DISCUSSION

A. XAS with potential modulation method

The *in operando* XAS measurement of the electrochemical reaction has been performed by the potential modulation

method as above described. The sample electrolyte is 0.5 M aqueous iron sulfate at $\text{pH} = 2.2$. The temperature of the electrolyte is 27°C . The change in valence of Fe ions in the electrochemical reaction of aqueous iron sulfate solution is measured by the Fe L-edge XAS. The photon energy resolution was set to 0.7 eV. The oxidation of Fe(II) to Fe(III) ions is occurred when the potential is increased, and the reduction of Fe(III) to Fe(II) ions is occurred when the potential is decreased.^{11,34–38}

Figure 2 shows the changes of the potential and the soft X-ray transmission signals, which are measured in the potential modulation at a fixed photon energy. The scan rate of the potential is 100 mV/s, the same as in CV. Figure 2(a) shows the electrode potential versus Ag/AgCl with saturated KCl solutions. The potential is increased from 0.0 V to 1.0 V after receiving the trigger signal, then decreased to -0.4 V, and increased to 0.0 V again. The one cycle of the potential modulation takes 28 s. Figure 2(b) shows the changes of the soft X-ray transmission during the potential modulation at the different photon energy measured by the multichannel scaler. The dwell time was set to 0.5 s, which corresponds to the potential step of 0.05 V. The soft X-ray transmission at 705 eV is not changed at different potentials because it is the region before the Fe L-edge. The absorption of Fe(II) ions is maximum at the photon energy of 708 eV. The transmission is increased when the potential is increased, and shows a maximum value at 10 s, which corresponds to the potential of 1.0 V. Then, it is decreased again in the downward potential after 10 s. On the other hand, the transmission at 710 eV is decreased in the upward potential, and is increased in the downward potential, because the absorption of Fe(III) ions is maximum at 710 eV. The photon energy of 713 eV is the region after the edge-jump. The transmission is slightly decreased in the upward potential due to the formation of Fe(III) ions.

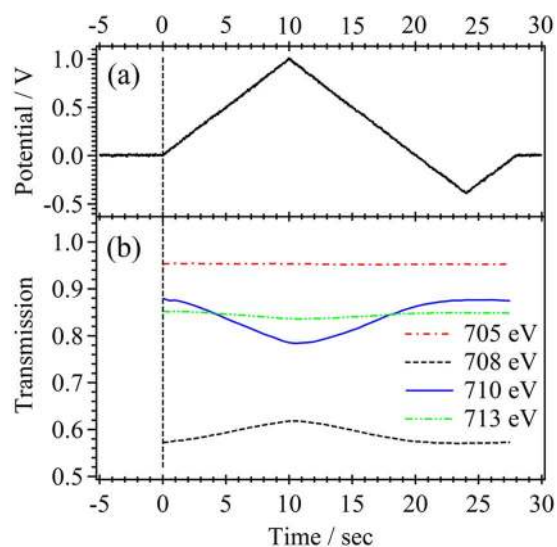


FIG. 2. Changes in soft X-ray transmission observed by modulating the potential of the electrodes at a fixed photon energy. One cycle of the potential modulation takes 28 s at 100 mV/s. Both the modulation of potentials and the measurement of soft X-ray transmission are started at 0 s. (a) The potential versus Ag/AgCl with saturated KCl solutions and (b) the soft X-ray transmission at several photon energies as a function of time.

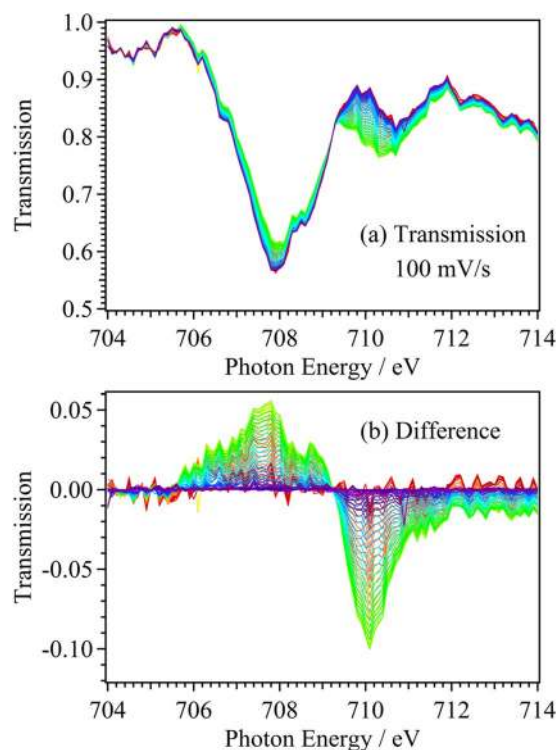


FIG. 3. (a) Soft X-ray transmission spectra at different potentials at a scan rate of 100 mV/s. (b) Difference spectra at different potentials from the Fe(II) spectra obtained at -0.4 V.

Figure 3(a) shows the changes of soft X-ray transmission with potential modulation as a function of photon energy, in which several changes of transmission signals are shown in Fig. 2(b). The intensities at the peaks of Fe(II) ions (708 eV) and Fe(III) ions (710 eV) are changed at different potentials. Figure 3(b) shows the difference spectra of soft X-ray transmission at different potentials from that at -0.4 V, where Fe(II) ions only exist by the reduction of Fe(III). The intensities of the Fe(II) and Fe(III) ions are changed continuously at different potentials. The isosbestic points are found at 709.2 eV, which is consistent with the previous study.¹¹ It means that only Fe(II) and Fe(III) ions are involved in the Fe redox reaction.

In the soft X-ray absorption coefficients $\ln(I_0/I)$, the intensity I_0 is for pure liquid water and is measured at the dwell time of 5 s by the NIM counter and is averaged over several measurements. The reference Fe L-edge XAS spectrum of Fe(II) ions was measured at no applied potential, whereas that of Fe(III) ions was obtained at an applied potential of 0.8 V after inducing 1.0 V during 1 min. The intensities I for the reference spectra are measured at the dwell time of 5 s by the NIM counter and are averaged over several measurements. Figure 4 shows the reference XAS spectra of Fe(II) and Fe(III) ions. These spectra are consistent with the previous studies.^{11,29–31}

For *in operando* XAS spectra of the electrochemical reaction, the intensities I at different potentials are obtained by summation of the reference soft X-ray transmission of Fe(II) ions and the difference spectra at different potentials from Fe(II) shown in Fig. 3(b), which are normalized for the

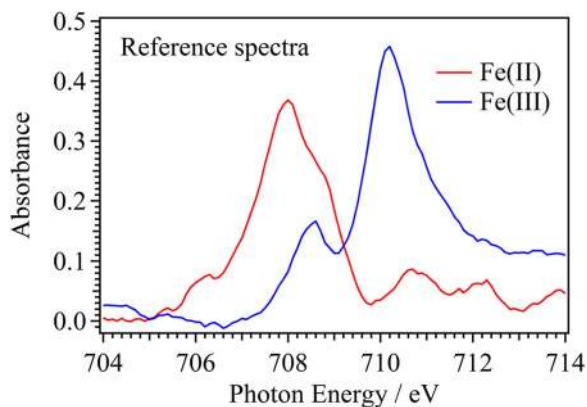


FIG. 4. Reference Fe L-edge XAS spectra for Fe(II) and Fe(III) ions in aqueous iron sulfate solutions.

same dwell time. The intensities I_0 is for pure liquid water. Figure 5(a) shows three-dimensional plots of Fe L-edge XAS spectra for the electrochemical reaction of iron sulfate solution at 100 mV/s. By increasing the potential from 0.0 V to 1.0 V, the peak intensity of Fe(II) is decreased and that of Fe(III) is increased. When the potential is decreased from 1.0 V to -0.4 V, the peak intensity of Fe(II) is increased

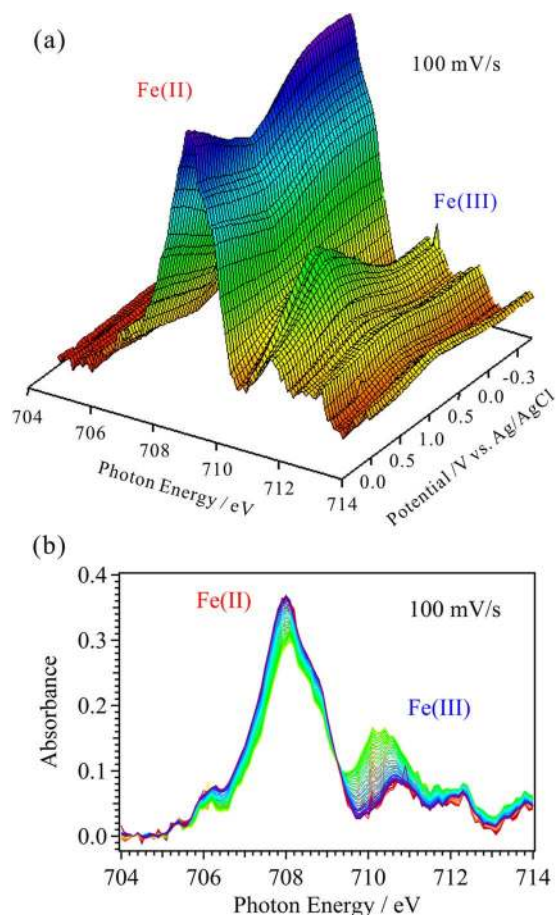


FIG. 5. (a) Three-dimensional plots of the Fe L-edge XAS spectra in the electrochemical reaction of aqueous iron sulfate solution at 100 mV/s. One axis is photon energy, and the other is the applied potential versus Ag/AgCl. (b) Fe L-edge XAS spectra at the potential step of 0.05 V in the electrochemical reaction shown in (a).

and that of Fe(III) is instead decreased. Figure 5(b) shows the Fe L-edge XAS spectra during the electrochemical reaction at the potential step of 0.05 V taken from Fig. 5(a). The isosbestic point is found at 709.2 eV, and the intensities of Fe(II) and Fe(III) ions are changed continuously at different potentials. Previously, the XAS spectra at constant potentials need long acquisition time and it is difficult to observe small spectral changes in electrochemical reactions. The potential-modulated XAS measurement enables us to investigate a subtle spectral change in the electrochemical reaction.

To obtain the fraction of Fe(II) and Fe(III) ions, we fit the Fe L-edge XAS spectra at different potentials to a superposition of the reference spectra of Fe(II) and Fe(III) ions shown in Fig. 4. Figure 6 shows an example of the least-squares fitting for the Fe L-edge XAS spectrum measured at a potential of 0.95 V in the downward scan direction and it is in good agreement with a simple superposition of the two reference spectra.

B. Rate dependence of Fe redox reaction

Figure 7(a) shows the CV spectra of aqueous iron sulfate solution at 100 mV/s. The oxidation of Fe(II) to Fe(III) ions with increasing potential is observed as the peak at 0.76 V. The reduction of Fe(III) to Fe(II) ions with decreasing potential is observed as the peak at 0.19 V.

In order to compare the CV spectra with the XAS spectra, we obtain the fraction of Fe(II) and Fe(III) ions by fitting the XAS spectra as shown in Fig. 6. Figure 7(b) shows change in valence of Fe ions in aqueous iron sulfate solution during the electrochemical reaction at 100 mV/s. The error of the fraction at 100 mV/s is within $\pm 2\%$. By increasing the potential from 0.0 V to 1.0 V, the fraction of Fe(II) ions decreases and that of Fe(III) ions increases. The fraction of Fe(III) at 1.0 V is 0.26. The Fe(II) ions are partially changed to the Fe(III) ions by the oxidation process. The central potentials of the Fe redox reaction are obtained by fitting the fraction change of Fe(III) ions with sigmoid profiles. The central potential of the oxidation process by increasing the potential is 0.59 V and that of the reduction process by decreasing the potential is 0.39 V. These potentials are different from that obtained

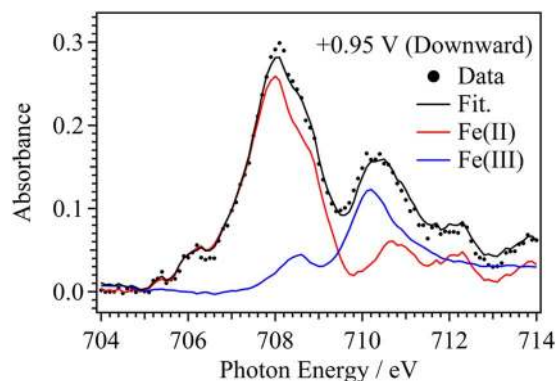


FIG. 6. Example of the fitting of the Fe L-edge XAS spectrum at the potential of 0.95 V in the downward scan direction by superposition of the two reference spectra.

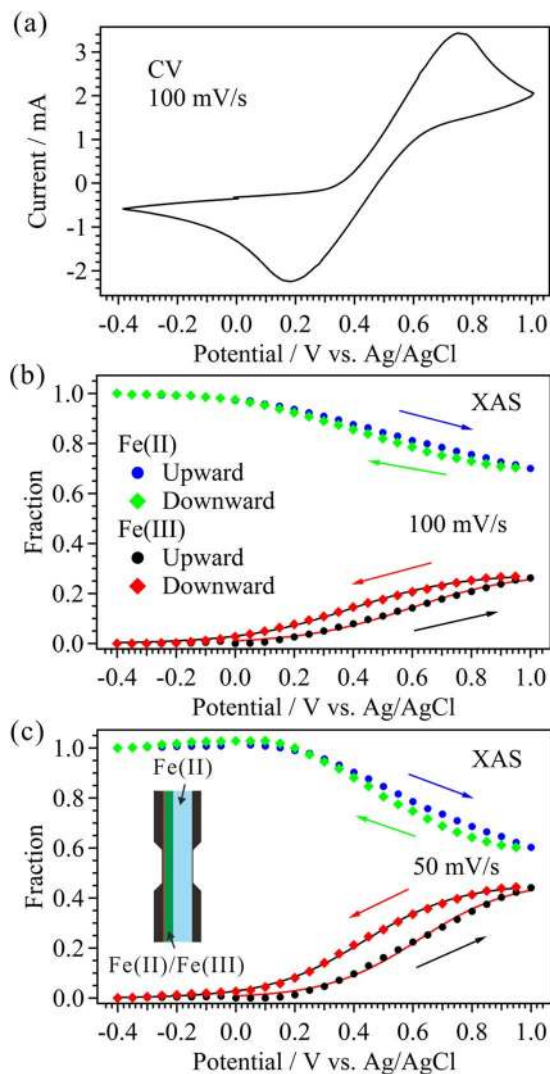


FIG. 7. (a) CV spectra of aqueous iron sulfate solution at 100 mV/s. Fractions of Fe(II) and Fe(III) ions as a function of potential versus Ag/AgCl in the electrochemical reaction of iron sulfate solutions at the scan rates of (b) 100 mV/s and (c) 50 mV/s. The inset shows that the liquid layer consists of the solid-liquid interface of the gold electrode and the bulk electrolyte of Fe(II) ions.

by CV at 100 mV/s: The central potential of the oxidation process obtained by XAS is lower than that obtained by CV, and the central potential of the reduction process obtained by XAS is higher than that obtained by CV.

Figure 7(c) shows change in valence of Fe ions at 50 mV/s obtained by the potential-modulated XAS. The error of the fraction at 50 mV/s is within $\pm 4\%$. The fraction of Fe(III) at 1.0 V is 0.44, and is larger than that at 100 mV/s. The central potentials of the oxidation and the reduction processes at 50 mV/s are 0.62 V and 0.43 V, respectively. These central potentials are not different from those at 100 mV/s.

The current peaks in CV reflect changes in valence of Fe ions at the solid-liquid interface of a gold electrode. As shown in the inset of Fig. 7, on the other hand, the XAS spectra include both the solid-liquid interface and the bulk electrolyte. The change in valence of Fe ions in the bulk electrolyte is influenced by the diffusion of Fe ions in the solution. When the scan rate is fast, the fraction change of Fe ions in the bulk

electrolyte is slower than that at the solid-liquid interface. That is why the central potentials in the upward scan direction obtained by XAS are lower than those obtained by CV, and the central potentials in the downward potentials obtained by XAS are higher than those obtained by CV. The diffusion of Fe ions also explains that the maximum fraction of Fe(III) ions at 50 mV/s is larger than that at 100 mV/s.

Recently, we have obtained the central potential of Fe redox reaction by measuring XAS at 0.08 mV/s, in which each XAS spectrum is measured at a constant potential.¹¹ In this condition, all the Fe(II) ions are changed to the Fe(III) ions by the oxidation process. The central potentials of both the simple oxidation and reduction processes obtained by XAS are consistent with those obtained by CV at 20 mV/s. Because of the slow scan rate, the diffusion of Fe ions does not affect the Fe redox reaction in the bulk electrolytes at 0.08 mV/s.

IV. SUMMARY

The local structures of liquid electrolytes and solid-liquid interfaces at electrodes in the electrochemical reaction are investigated by a newly developed *in operando* XAS measurement system at the scan rate of 100 mV/s, which is the same as in CV. The XAS measurement is performed by using a transmission-type liquid flow cell with built-in electrodes. The electrode potential is swept with the scan rate of 100 mV/s at a fixed photon energy and soft X-ray absorption coefficients at different potentials are measured at the same time. By repeating the potential modulation at every photon energy, it is possible to obtain the XAS spectra of electrochemical reaction at 100 mV/s.

By measuring the Fe L-edge XAS spectra at 100 mV/s, we have investigated change in valence of Fe ions in the electrochemical reaction of aqueous iron sulfate solutions. In the oxidation process by increasing the potential, the maximum fraction of the Fe(III) ions is only 0.26. The central potentials of both the oxidation and reduction processes obtained by XAS are different from those obtained by CV. The Fe redox reaction at 50 mV/s also shows the same feature. The current peaks in CV reflect the Fe redox reaction at the solid-liquid interface; on the other hand, the XAS spectra include both the solid-liquid interface and the bulk electrolyte. The change in valence of Fe ions in the bulk electrolyte is influenced by the diffusion of Fe ions, and the central potentials are dependent with the scan rate. The XAS for different thickness of the liquid layer may distinguish the change in valence of Fe ions at the solid-liquid interface and in the bulk electrolyte.

The liquid cell for XAS has given a chance to reveal the local structures of liquid and aqueous solution, such as hydrogen bond of water in liquid water¹⁻³ and hydrophobic interaction of methanol in aqueous methanol solution.³³ The present *in operando* electrochemical cell opens a possibility to reveal the adsorption structural change of water molecules in electric double layers at different potentials by using O K-edge XAS for electrochemical reactions, such as aqueous sulfuric acid solutions on platinum electrodes.

ACKNOWLEDGMENTS

This work is supported by JSPS Grant-in-Aid for Scientific Research (Grant Nos. 23685006 and 23245007). We acknowledge the staff members of the UVSOR-III facility for their kind support.

- ¹J. D. Smith, C. D. Cappa, K. R. Wilson, B. M. Messer, R. C. Cohen, and R. J. Saykally, *Science* **306**, 851 (2004).
- ²P. Wernet, D. Nordlund, U. Bergmann, M. Cavalleri, M. Odellius, H. Ogasawara, L.-Å. Näslund, T. K. Hirsch, L. Ojamäe, P. Glatzel, L. G. M. Pettersson, and A. Nilsson, *Science* **304**, 995 (2004).
- ³C. Huang, K. T. Wikfeldt, T. Tokushima, D. Nordlund, Y. Harada, U. Bergmann, M. Niebuhr, T. M. Weiss, Y. Horikawa, M. Leetmaa, M. P. Ljungberg, O. Takahashi, A. Lenz, L. Ojamäe, A. P. Lyubartsev, S. Shin, L. G. M. Pettersson, and A. Nilsson, *Proc. Natl. Acad. Sci. U.S.A.* **106**, 15214 (2009).
- ⁴M. Nagasaka, T. Hatsui, T. Horigome, Y. Hamamura, and N. Kosugi, *J. Electron Spectrosc. Relat. Phenom.* **177**, 130 (2010).
- ⁵S. Schreck, G. Gavrilu, C. Weniger, and P. Wernet, *Rev. Sci. Instrum.* **82**, 103101 (2011).
- ⁶A. J. Achkar, T. Z. Regier, H. Wadati, Y.-J. Kim, H. Zhang, and D. G. Hawthorn, *Phys. Rev. B* **83**, 081106(R) (2011).
- ⁷M. D. Gotz, M. A. Soldatov, K. M. Lange, N. Engel, R. Golnak, R. Könnecke, K. Atak, W. Eberhardt, and E. F. Aziz, *J. Phys. Chem. Lett.* **3**, 1619 (2012).
- ⁸T. Z. Regier, A. J. Achkar, D. Peak, J. S. Tse, and D. G. Hawthorn, *Nat. Chem.* **4**, 765 (2012).
- ⁹M. A. Soldatov, K. M. Lange, M. D. Gotz, N. Engel, R. Golnak, A. Kothe, and E. F. Aziz, *Chem. Phys. Lett.* **546**, 164 (2012).
- ¹⁰C. T. Chantler, *J. Phys. Chem. Ref. Data* **29**, 597 (2000).
- ¹¹M. Nagasaka, H. Yuzawa, T. Horigome, A. P. Hitchcock, and N. Kosugi, *J. Phys. Chem. C* **117**, 16343 (2013).
- ¹²O. Endo, M. Kiguchi, T. Yokoyama, M. Ito, and T. Ohta, *J. Electroanal. Chem.* **473**, 19 (1999).
- ¹³D. K. Bora, P.-A. Glans, J. Pepper, Y.-S. Liu, C. Du, D. Wang, and J.-H. Guo, *Rev. Sci. Instrum.* **85**, 043106 (2014).
- ¹⁴T. Masuda, H. Yoshikawa, H. Noguchi, T. Kawasaki, M. Kobata, K. Kobayashi, and K. Uosaki, *Appl. Phys. Lett.* **103**, 111605 (2013).
- ¹⁵K. Ashley and S. Pons, *Chem. Rev.* **88**, 673 (1988).
- ¹⁶M. Nakamura, H. Kato, and N. Hoshi, *J. Phys. Chem. C* **112**, 9458 (2008).
- ¹⁷S. Nihonyanagi, S. Ye, K. Uosaki, L. Dreesen, C. Humbert, P. Thiry, and A. Peremans, *Surf. Sci.* **573**, 11 (2004).
- ¹⁸B. Pettinger, M. R. Philpott, and J. G. Gordon II, *Surf. Sci.* **105**, 469 (1981).
- ¹⁹M. F. Toney, J. N. Howard, J. Richer, G. L. Borges, J. G. Gordon, O. R. Melroy, D. G. Wiesler, D. Yee, and L. B. Sorensen, *Nature (London)* **368**, 444 (1994).
- ²⁰S. Wu, J. Lipkowski, T. Tylliszczak, and A. P. Hitchcock, *Prog. Surf. Sci.* **50**, 227 (1995).
- ²¹S. Wu, Z. Shi, J. Lipkowski, A. P. Hitchcock, and T. Tylliszczak, *J. Phys. Chem. B* **101**, 10310 (1997).
- ²²D. Guay, J. Stewart-Ornstein, X. Zhang and A. P. Hitchcock, *Anal. Chem.* **77**, 3479 (2005).
- ²³B. Bozzini, A. Gianoncelli, P. Bocchetta, S. Dal Zilio, and G. Kourousias, *Anal. Chem.* **86**, 664 (2014).
- ²⁴K. Ataka, T. Yotsuyanagi, and M. Osawa, *J. Phys. Chem.* **100**, 10664 (1996).
- ²⁵K. Kunimatsu, H. Hanawa, H. Uchida, and M. Watanabe, *J. Electroanal. Chem.* **632**, 109 (2009).
- ²⁶J. Wang, B. M. Ocko, A. J. Davenport, and H. S. Isaacs, *Phys. Rev. B* **46**, 10321 (1992).
- ²⁷M. Nakamura, O. Endo, T. Ohta, M. Ito, and Y. Yoda, *Surf. Sci.* **514**, 227 (2002).
- ²⁸B. Braunschweig, P. Mukherjee, D. D. Dlott, and A. Wieckowski, *J. Am. Chem. Soc.* **132**, 14036 (2010).
- ²⁹A. P. Hitchcock, A. T. Wen, and E. Rühl, *Chem. Phys.* **147**, 51 (1990).
- ³⁰G. Cressey, C. M. B. Henderson, and G. Van der Laan, *Phys. Chem. Miner.* **20**, 111 (1993).
- ³¹K. M. Lange, A. Kothe, and E. F. Aziz, *Phys. Chem. Chem. Phys.* **14**, 5331 (2012).
- ³²T. Hatsui, E. Shigemasa, and N. Kosugi, *AIP Conf. Proc.* **705**, 921 (2004).
- ³³M. Nagasaka, K. Mochizuki, V. Leloup, and N. Kosugi, *J. Phys. Chem. B* **118**, 4388 (2014).
- ³⁴R. E. Huffman and N. Davidson, *J. Am. Chem. Soc.* **78**, 4836 (1956).
- ³⁵J. Beukenkamp and K. D. Herrington, *J. Am. Chem. Soc.* **82**, 3022 (1960).
- ³⁶M. Iwai, H. Majima, and Y. Awakura, *Metall. Mater. Trans. B* **13**, 311 (1982).
- ³⁷A. F. Gil, L. Salgado, L. Galicia, and I. González, *Talanta* **42**, 407 (1995).
- ³⁸A. F. Gil, L. Galicia, and I. González, *J. Electroanal. Chem.* **417**, 129 (1996).